Néel-type domain wall excitation in perpendicular magnetization thin films

N. Vukadinovic
Dassault Aviation, 92 552 St-Cloud, France

J. Ben Youssef
LMB, CNRS-UMR 6135, 29285 Brest, France

M. Labrune
LPMTM, CNRS, Université Paris 13, 93430 Villetaneuse, France

(Received 20 August 2002; published 31 October 2002)

Domain wall (DW) magnetic excitations in perpendicular magnetization thin films with a stripe domain structure are investigated by means of a two-dimensional dynamic micromagnetic model. A thickness dependent Néel-type DW mode is evidenced for the longitudinal exciting configuration. The numerical dynamic susceptibility spectra are first compared with those deduced from the extended wall-wave model of Slonczewski, and are then nicely correlated with zero-field domain wall resonance measurements.

DOI: 10.1103/PhysRevB.66.132418 PACS number(s): 75.60.Ch, 75.40.Gb, 75.70.−i, 76.50.+g

The small amplitude spin dynamics of nonuniform magnetization distributions is a very attractive topic driven both by basic research and potential applications in future storage media and microwave devices.[1] In this context, the periodic stripe domains which appear in thin magnetic films with a perpendicular anisotropy represent a model system. The high-frequency spin dynamics of thin films with a low perpendicular anisotropy ($Q<1$, where Q is the quality factor defined as $Q=K_U/2\pi M_S^2$, with K_U the uniaxial anisotropy constant and M_S the saturation magnetization) supporting a weak stripe domain structure[2] was recently studied both experimentally and theoretically.[3–7] As a conclusion, the experimental dynamic spectra exhibit multiple resonances which are strongly dependent on the equilibrium micromagnetic state and on the rf exciting field orientation. Dynamic micromagnetic simulations permitted one to reproduce complex zero-field microwave permeability spectra[5] and to identify some excitations observed in ferromagnetic resonance (FMR) measurements.[7] For thin films with a large perpendicular anisotropy ($Q>1$), possessing nearly homogeneous domains with alternatively up-and-down magnetizations separated by narrow domain walls (DW's),[8] numerous studies were devoted to domain wall resonances (DWR's).[9–12] One of the main results is the existence of high-order DWR's interpreted by Slonczewski in terms of flexural domain wall (FDW) modes. His wall-wave model (FDW model) (Ref. 9) correctly described the experimental in-plane dc field[11] and thickness[12] dependences of the DWR frequencies. However, a large discrepancy subsists concerning the high-frequency FDW resonance for the thinnest films.[12] In addition, the theoretical relative FDW mode intensities differ from the experimental ones.[10] Lastly, the effect of the rf exciting field orientation on the zero-field DWR spectra has never been quantitatively addressed.

The purpose of this paper is to revisit, by means of a two-dimensional (2D) dynamic micromagnetic model, the small amplitude DW excitations occurring in perpendicular magnetization thin films ($Q>1$) possessing a parallel stripe domain structure. Special attention is paid to the mode located within the Néel part of the DW, excited by the pumping field applied along the stripe direction, and experimentally evidenced.

The 2D dynamic micromagnetic model for computing the dynamic susceptibility tensor $\bar{\chi}$ is based on the solution in the frequency domain of the Landau-Lifshitz-Gilbert equation for magnetization motion linearized around the equilibrium configuration.[5,7] The magnetic system is assumed invariant along one direction (z axis), periodic along the second direction (x axis), and of finite thickness along the third direction (y axis). The computations were performed with the following magnetic parameters: $4\pi M_S=145$ G, $K_U=1150$ erg/cm^3, the exchange constant $A=1.5\ 10^{-7}$ erg/cm, the gyromagnetic ratio $\gamma=1.8\ 10^7$ Oe^{-1}s^{-1}, the Gilbert damping parameter $\alpha=0.02$, and the film thickness $h=1.5\ \mu$m, which are representative of a single-crystal garnet film. In order to ensure reliable micromagnetic simulations, a spatial discretization with mesh sizes $\Delta x \simeq \Delta_0/4$ and $\Delta y \simeq \Delta_0/2$ [$\Delta_0=(A/K_U)^{1/2}$ is the Bloch DW width parameter] were used for this sample with $Q=1.38$.

The static DW structure in the periodic stripe domain pattern (zero-field period P_0) is displayed in Fig. 1 within the restricted cross-sectional area $[-P_0/12,P_0/12]\times[0,h]$ [Fig. 1(a)]. Domains magnetized, respectively, along the $+y$ axis (red area) and the $-y$ axis (blue area) are observed, separated by a DW which is shrinked in the film center. A so-called twisted DW with a Bloch character in the film center and a Néel character at the film surfaces is observed. The corresponding DW magnetization in-plane (or twist) angle, denoted ψ_0, is plotted as a function of the reduced coordinate y/h (solid line) in Fig. 1(b) and compared with the one computed from the Slonczewski's model in which the DW is considered as a zero-thickness membrane ($Q\gg1$).[8] For this sample with a moderate DW aspect ratio $h/\pi\Delta_0 \simeq 4$, the micromagnetic computation leads to a larger ψ_0 value with respect to Slonczewski's formalism including a simplified computation of the DW demagnetizing field as discussed in Ref. 13.

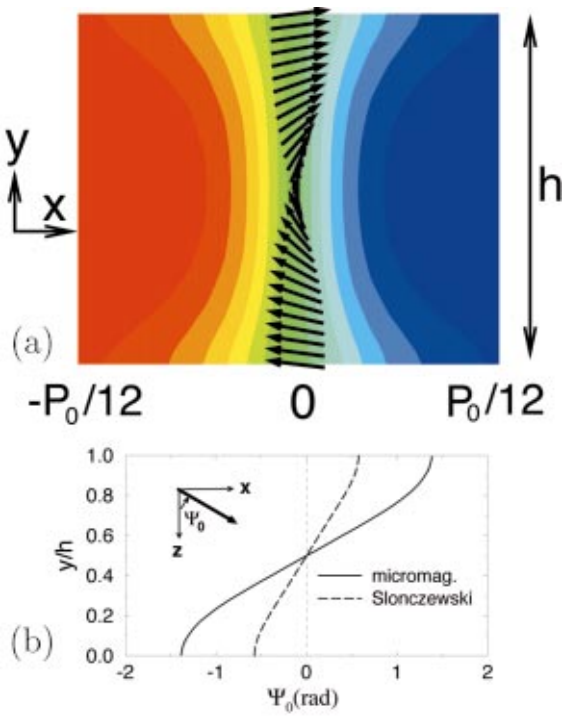

FIG. 1. (Color) Static DW structure in a periodic stripe domain pattern. (a) Micromagnetic computation of the equilibrium configuration. A color code images the normal magnetization component m_y. The positive values are in red, whereas the negative ones are in blue. The arrows represent the magnetization components in the plane (Ox,Oz) at the middle of the DW. (b) Static DW azimuthal angle ψ_0 along the film thickness.

The imaginary diagonal elements of the dynamic susceptibility tensor averaged over the periodic cell, χ''_{ii}, $i=x,y,z$ are displayed as a function of frequency in Fig. 2. The numerical spectra (solid line) exhibit two resonances both for χ''_{xx} and χ''_{yy}, and one resonance for χ''_{zz}. The color insets correspond to respective imaginary local susceptibility tensor element, $\chi''_{ii}(x,y)$, $i=x,y,z$ at each resonance frequency. For χ''_{xx} [Fig. 2(a)], the low-frequency resonance, noted (1), arises mainly from the spins located within the Bloch part of the DW due to the coupling between the exciting field $\delta h_{rf,x}$ and the predominant static DW magnetization component m_z. In this case, the imaginary local susceptibility is always positive. For the high-frequency resonance, noted (2), the important levels of the imaginary local susceptibility are dominantly found within the DW, but in contrast to resonance (1), the sign of the imaginary local susceptibility alternates from negative to positive and again negative through the film thickness. Resonances (1) and (2) are observed at the same frequencies for χ''_{yy} [Fig. 2(b)], but the intensity of resonance (1) is increased whereas that of resonance (2) is drastically reduced. The map of the local susceptibilities indicates that all the spins of the DW contribute to these resonances due to the coupling between $\delta h_{rf,y}$ and the static DW magnetization in-plane components m_x and m_z. Similarly to the χ''_{xx} element, the sign of the local susceptibility remains positive for resonance (1) and varies from negative to positive and conversely along the film thickness for resonance

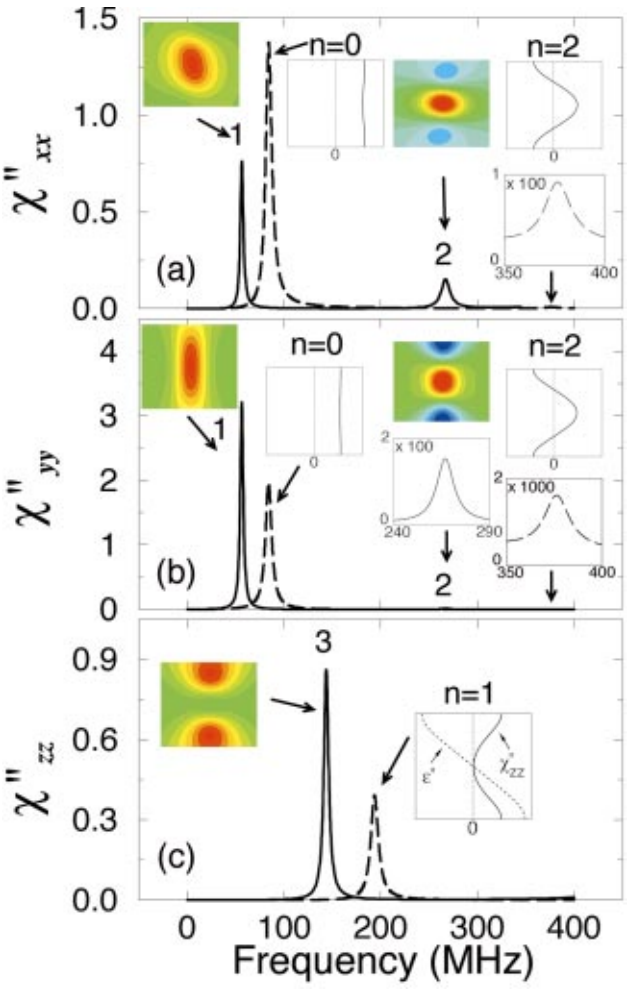

FIG. 2. (Color) Imaginary part of the diagonal elements of the dynamic susceptibility tensor as a function of frequency: (a) χ''_{xx}, (b) χ''_{yy}, and (c) χ''_{zz}. The solid lines correspond to the 2D dynamic micromagnetic simulations. The color maps represent the spatial distribution of the respective susceptibility tensor element (imaginary part) at each resonance frequency. The coordinate system, the boundaries of maps, and the color code are the same as in Fig. 1(a). The dashed lines display the FDW dynamic susceptibility spectra. For each flexural mode, the *y* dependence of the dynamic susceptibility (imaginary part) is plotted in insets. The insets labeled with magnification factors correspond to weak signals.

(2). A noticeable result is the existence of an intensive resonance, noted (3), at 143 MHz for the χ''_{zz} spectrum [Fig. 2(c)]. This absorption line results from the excitation of spins located within the Néel parts of the DW, as demonstrated by the local susceptibility map.

It is instructive to compare these dynamic responses with those computed by using the FDW model based on the Slonczewski equations (limit of large Q).[8] The DW dynamics is then described by two degrees of freedom: q, the wall displacement in the x direction; and ψ, the azimuthal angle of the magnetization **M** evaluated at the middle of the wall from the z axis. For parallel stripe domains, the FDW model treats small amplitude DW oscillations about the equilibrium depending on the coordinate y along the film normal and on a wave vector **k** parallel to the film plane. These FDW exci-

tations are distinguished by the number of nodes n in the y dependence of q. By considering only the uniform mode oscillations ($k_z=0$, $k_x=\pm 2\pi/P_0$),[10] the diagonal elements of the dynamic susceptibility tensor averaged over the whole thickness have been computed by extending the procedure described in Ref. 12, and are given by

$$\chi_{xx}=\frac{\langle \epsilon(\xi)\ \cos\psi_0(\xi)\rangle}{8\ \delta\tilde{h}_{rf,\,x}},\quad \chi_{yy}=\frac{\Delta_0\langle \eta(\xi)\rangle}{\pi\ P_0\ \delta\tilde{h}_{rf,\,y}},$$

$$\chi_{zz}=-\frac{\langle \epsilon(\xi)\ \sin\psi_0(\xi)\rangle}{8\ \delta\tilde{h}_{rf,\,z}}, \tag{1}$$

with $\langle v(\xi)\rangle=\int_0^1 v(\xi)d(\xi)$ for any given function v, $\xi=y/h$, ϵ the amplitude of the dynamic azimuthal variation, $\epsilon=\Sigma_{\lambda=0}^{\infty} C_\lambda{}'\cos\pi\lambda\xi$, $q=\Delta_0\eta$, $\eta=\Sigma_{\lambda=0}^{\infty} C_\lambda\cos\pi\lambda\xi$, $\delta\tilde{h}_{rf,\,i}=\delta h_{rf,\,i}/8M_S$, $i=x,z$, and $\delta\tilde{h}_{rf,\,y}=\delta h_{rf,\,y}/4\pi M_S$. The coefficients C_λ and $C_\lambda{}'$ are the solutions of the linear system

$$\begin{bmatrix} \mathbf{B}+i\alpha\tilde{\omega}\mathbf{I} & i\tilde{\omega}\mathbf{I} \\ i\tilde{\omega}\mathbf{I} & -(\mathbf{B}'+i\alpha\tilde{\omega}\mathbf{I}) \end{bmatrix}\begin{bmatrix} \mathbf{C} \\ \mathbf{C}' \end{bmatrix}=\begin{bmatrix} \mathbf{H^n} \\ \mathbf{H^t} \end{bmatrix}, \tag{2}$$

where the matrices $\mathbf{B}$ and $\mathbf{B}'$ depend on the static DW structure $\psi_0(\xi)$ and profiles of static and dynamic demagnetizing fields,[9,12] $\mathbf{I}$ is the unity matrix, and the vectors $\mathbf{H}^n$ and $\mathbf{H}^t$ are related, respectively, to the normal and in-plane components of the exciting field $\delta\mathbf{h}_{rf}$. In practice, system (2) truncated at 32×32 ($\mathbf{B},\mathbf{B}'$, and $\mathbf{I}$ are 16×16 matrices and $\mathbf{C},\mathbf{C}',\mathbf{H^n}$, and $\mathbf{H^t}$ are vectors of size 16) is solved for each reduced angular frequency $\tilde{\omega}$, $\omega=4\pi\gamma M_S\tilde{\omega}$.

The dynamic susceptibility spectra computed by the FDW model are also reported in Fig. 2 (dashed line). With respect to the micromagnetic simulations, several comments can be made: (i) three resonances ($n=0$, 1, 2) are also predicted by the FDW model, but the resonance frequencies are shifted towards higher frequencies. (ii) The intensities of the $n=0$ and 1 modes are, respectively, of the same order of magnitude than those of resonances (1) and (3). In contrast, the intensity of the $n=2$ mode is one order of magnitude weaker with respect to the resonance (2). (iii) The reduced resonance linewidths $\Delta f_r/f_r$ (full width at half maximum Δf_r and resonance frequency f_r) exceed by about 50% those computed by the micromagnetic model. (iv) The local susceptibility profiles $\chi''_{ii}(y)$, $i=x,y,z$ (insets in Fig. 2) computed by the FDW model are in qualitative agreement with those deduced from the micromagnetic simulations and evaluated at the middle of the DW. For the $n=2$ mode, the position of the two nodes along the y axis is very close to the one computed for resonance (2). The dynamic azimuthal variation ϵ ($\epsilon=\epsilon'-i\epsilon''$) is an odd function with respect to the film center (mode $n=1$), but the local susceptibility is an even function in agreement with the micromagnetic simulations [resonance (3)].

Let us focus on the Néel-type DW resonance (3). Figure 3 shows the numerical χ''_{zz} spectrum for different film thicknesses. Increasing film thickness yields a decrease both of the resonance frequency and line intensity. The FDW model (inset in Fig. 3) also predicts a rapid decrease of the resonance frequency for the $n=1$ mode with increasing film thickness, but the resonance frequencies are overestimated with respect to the dynamic micromagnetic model. In this thickness range, the resonance frequencies of the $n=0$ and 2 modes also decrease with increasing film thickness.[12]

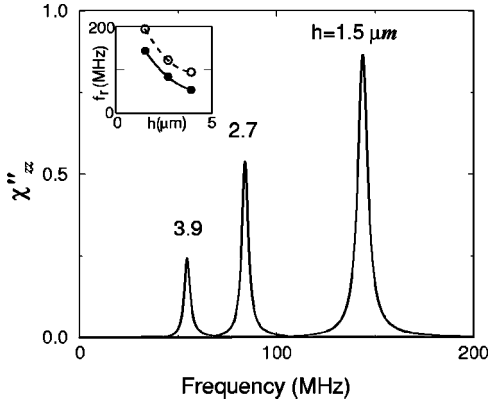

FIG. 3. Imaginary part of the dynamic susceptibility tensor element χ''_{zz} as a function of frequency for various film thicknesses. The resonance line is associated with the Néel-type DW mode. The inset represents the thickness dependence of the resonance frequency computed by the dynamic micromagnetic model (full circles) and by the FDW model (open circles).

These 2D dynamic micromagnetic simulations have been compared with DWR measurements performed over the frequency range 0–300 MHz by using a wideband resonance spectrometer with nonresonant microstrip transmission line. The investigated sample is a single-crystal garnet film $Y_{2.86}La_{0.12}Fe_{3.82}Ga_{1.18}O_{12}$ grown by liquid phase epitaxy on a (111)-oriented substrate of gadolinium gallium garnet. The material parameters correspond to those used in the dynamic susceptibility computations except the damping parameter. The parallel stripe domains were generated after a special field treatment.[14] The experimental P_0 value ($P_0\simeq 4.3\ \mu$m) measured by means of a polarizing microscope was found to be in very good agreement with the one deduced from static micromagnetic simulations ($P_0=4.4\ \mu$m). Figure 4 displays the theoretical and experimental derivative rf power absorptions dP_a/df versus frequency for two orientations of stripe domains with respect to the microstrip line, respectively, parallel [Fig. 4(a)] and perpendicular [Fig. 4(b)] to it. Due to the microstrip line symmetry, the exciting field $\delta\mathbf{h}_{rf}$ possesses two components for each pumping configuration; a large in-plane one perpendicular to the microstrip line (x or z axis) and a weaker one perpendicular to the film (y axis). The experimental spectra reveal clearly two magnetic resonances for each exciting configuration. The theoretical microwave power P_a absorbed per unit volume is computed from the general expression

$$P_a=\left\langle \left\langle \delta\mathbf{h}_{rf}\cdot\frac{d\mathbf{m}}{dt}\right\rangle_{\text{cell}}\right\rangle_{\text{timeaverage}},$$

where $\langle\ \rangle_{cell}$ means spatial average over the periodic cell. A very good agreement is found between the experimental and

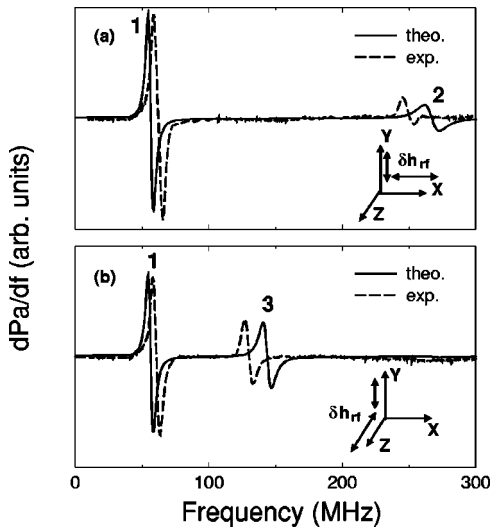

FIG. 4. Comparison between computed (solid lines) and experimental (dashed lines) zero-field DWR derivative spectra for a single-crystal garnet film: (a) stripe domains parallel to the microstrip line (z axis), and (b) stripe domains (z axis) perpendicular to the microstrip line (x axis).

theoretical line positions which allows an unambiguous assignment of the experimental lines. In particular, the high-frequency resonance observed for stripe domains perpendicular to the microstrip line, corresponds to the Néel-type DW mode. It must be mentioned that the theoretical spectra were computed by using a Gilbert damping parameter value $\alpha = 0.036$ far in excess with respect to the one deduced from FMR measurements performed over the frequency range 6–12 GHz in the saturated state (frequency dependence of the perpendicular resonance field), $\alpha = 0.002$. This questions once again the validity of the phenomenological Gilbert dissipation term. Though different explanations were proposed for interpreting such discrepancies [the effect of the relaxational dynamics of the magnetization modulus,[15,16] the frequency dependence of α (Ref. 13)], this problem still remains open.

In summary, DW magnetic excitations in perpendicular magnetization thin films with a stripe domain structure were investigated by using a 2D dynamic micromagnetic model. The orientation of the rf pumping field with respect to the stripe direction determines the selection rules for excitation of the three possible DW modes. For the longitudinal configuration (pumping field along the stripe direction), a Néel-type DW mode is clearly pointed out whose features were analyzed in the (thickness, frequency) plane. The analytical FDW model of Slonczewski also predicts three DW modes and provides a good estimation of the thickness dependence of the Néel-type DWR frequency. However, significant discrepancies (line positions, intensities, linewidths) exist with respect to the micromagnetic simulations. Experimental zero-field DWR spectra performed on a single-crystal garnet film are very nicely reproduced by the dynamic micromagnetic model, provided that the damping parameter is suitably chosen.

[1] G. Hillebrands and K. Ounadjela, *Spin Dynamics in Confined Magnetic Structures*, (Springer, London, 2002), Vol. 1.
[2] A. Hubert and R. Schaefer, *Magnetic Domains* (Springer, London, 1998).
[3] O. Acher, C. Boscher, G. Perrin, N. Vukadinovic, G. Suran, and H. Joinsten, J. Appl. Phys. **81**, 4057 (1997).
[4] U. Ebels, P.E. Wigen, and K. Ounadjela, Europhys. Lett. **46**, 94 (1999).
[5] N. Vukadinovic, O. Vacus, M. Labrune, O. Acher, and D. Pain, Phys. Rev. Lett. **85**, 2817 (2000).
[6] U. Ebels, L. Buda, K. Ounadjela, and P.E. Wigen, Phys. Rev. B **63**, 174437 (2001).
[7] N. Vukadinovic, M. Labrune, J. Ben Youssef, A. Marty, J.C. Toussaint, and H. Le Gall, Phys. Rev. B **65**, 054403 (2002).
[8] A.P. Malozemoff and J.C. Slonczewski, *Magnetic Domain Walls in Bubble Materials* (Academic, New York, 1979).
[9] J.C. Slonczewski, J. Magn. Magn. Mater. **23**, 305 (1981).
[10] B.E. Argyle, W. Jantz, and J.C. Slonczewski, J. Appl. Phys. **54**, 3370 (1983).
[11] S. Batra and P.E. Wigen, J. Appl. Phys. **61**, 4207 (1987).
[12] N. Vukadinovic, A. Serraj, H. Le Gall, and J. Ben Youssef, Phys. Rev. B **58**, 385 (1998).
[13] A. Thiaville, J. Miltat, and J. Ben Youssef, Eur. Phys. J. B **23**, 37 (2001).
[14] H. Le Gall, N. Vukadinovic, J. Ostorero, and J.M. Desvignes, J. Magn. Magn. Mater. **84**, 229 (1990).
[15] V.G. Bar'yakhtar, Zh. Éksp. Teor. Fiz. **87**, 1501 (1984) [Sov. Phys. JETP **60**, 863 (1984)].
[16] V.L. Sobolev, S.C. Chen, and H.L. Huang, J. Magn. Magn. Mater. **172**, 83 (1997).